Ground state of a dissipative two-level system

Han Rongsheng, Gao Xianlong, and Wang Kelin*
Department of Astronomy and Applied Physics and Center for Nonlinear Science, University of Science and Technology of China, Hefei 230026, People's Republic of China

Li Tongzhong
Department of Applied Physics, Shanghai Jiao Tong University, Shanghai, 200240, People's Republic of China
(Received 22 June 2000)

The ground state of a two-level system coupled to a dispersionless phonon bath is studied using the coherent approximation method. The ground-state energy and the tunneling reduction factor we obtain are in good agreement with the exact values in the whole parameter space. Since the real ground-state wave functions are well simulated, some other physical information about the system, such as the interaction energy and the interaction phonon numbers in each level and the whole system, are given. The interaction phonon numbers in the two-level system are found to increase with the coupling parameter s. In the intermediate coupling region, phenomenon of the population inversion and a maximum for the interaction phonon numbers versus δ_0/s have been found. Consisting with the exact results, our results show there is no evidence of the discontinuous localization-delocalization transition.

I. INTRODUCTION

The two-level system coupled to a phonon bath has extensive application in various fields of physics and chemistry,[1] such as molecular polaron formation, exciton motion, chaos in quantum, spin-phonon relaxation,[2] attenuation of sound in glasses,[3] the motion of defects in certain crystalline solids, and condensed matter physics. Many approximation methods have been applied to the system.[4–13] Ivić *et al.*[12] and Lo *et al.*[13] made use of the variational principle, and predicted the existence of the discontinuous localization-delocalization transition. Their prediction is contrary to the exact result that was obtained by Lo and Wong[14] via a combination of unitary transformations and numerical diagonalization. This fault maybe caused by the fact that variational calculations could not simulate the true ground state well. Fessatidis *et al.*[15] applied the Lanczos calculations to the system, while some other researchers used the connected moments expansion[16] (CMX) and the alternate moments expansion.[17] (AMX) Their results did not agree well with the exact solution when the coupling was strong. Recently, Wong and Lo applied a coupled-cluster approximation[18] (CCA) to this system with great success. The CCA method is needed to solve a number of coupled and, in general, nonlinear equations.

The two-level system coupled to a dissipative environment is defined by the Hamiltonian

$$\hat{H} = -\delta_0 \sigma_x + \sum_{\mathbf{k}} \hbar \omega_{\mathbf{k}} a_{\mathbf{k}}^{\dagger} a_{\mathbf{k}} + \sum_{\mathbf{k}} g_{\mathbf{k}} (a_{\mathbf{k}}^{\dagger} + a_{\mathbf{k}}) \sigma_z , \qquad (1)$$

where $a_{\mathbf{k}}$ and $a_{\mathbf{k}}^{\dagger}$ are boson annihilation and creation operators, respectively, and σ_x and σ_z are usual Pauli matrices. The bare tunneling matrix element is given by δ_0, while $g_{\mathbf{k}}$ represents the coupling to the $\mathbf{k}$ phonon mode. The first term in the right-hand side of Eq. (1) represents the tunneling effect, the second is the phonon energy, and the third is the interaction energy of the two-level system interacting with the phonon bath. For simplicity, we only consider the dispersionless case ($\omega_{\mathbf{k}} = \omega_0$ for all $\mathbf{k}$) in this paper. From the Hamiltonian (1), we can see that in the extreme case $\delta_0 = 0$, Eq. (1) represents a sets of oscillators. Thus there is a twofold degenerate localized ground state with energy $E = -s$. On the other hand, when the system is uncoupled ($g_{\mathbf{k}} = 0$), the eigenstate of the system are the symmetric and antisymmetric combinations of the spin states with energies $E_0 = \pm \delta_0$.

In the present work we introduce the coherent approximation (CA) to the two-level system coupled to a dispersionless phonon bath.[19–22] The CA is a nonvariational, nonperturbation method which provides a systematic scheme to improve the approximation of the system. The key idea of the CA is based on the fact that the interactions between the two-level system and the phonon bath consist of the effects of the one-phonon correlations, the two-phonon correlations, and so on. The effect of the N-phonon correlation will contribute little when N is big. So we can simulate the real system by just taking into account some rank of phonon correlations, for instance, two- or three-phonon correlations. These truncation schemes are similar to the Zubarev equation of motion decoupling schemes for Green's functions in which the higher-order correlation effects are averagely treated.[23] In this paper, the system is studied in a wide range of the parameter space. In the two-level approximation, the numerical results of the interaction phonon numbers and the interaction energy are obtained. In the intermediate region, we find that there exist an interesting phenomenon near the point $\delta_0/s \approx 0.5$. When δ_0/s increases across this point, the population of the interaction phonons invert. Also in this region, there is an existence of peaks in the curves of the interaction phonon numbers versus δ_0/s due to the strong nonlinear self-trapping effect. Consistent with the exact solution, we show no existence of the discontinuous localization-delocalization transition of the tunneling particle.

The present paper is organized as follows. In Sec. II we apply the CA to a two-state system coupled to a dispersionless bath. Numerical results are discussed in Sec. III. Finally a summary is given in Sec. IV.

II. COHERENT APPROXIMATION FOR A TWO-LEVEL SYSTEM WITH PHONON COUPLING

From the Hamiltonian $\hat{H}$, we can see that the two-level system coupled linearly to the phonon bath and the number of the phonons is nonconservative. Therefore it is appropriate to write the ground-state wave function of the two-level system in the coherent-state space.

In the first level approximation, we omit the two-phonon and more higher-order correlation terms and suppose the ground state of a many-body Hamiltonian $\hat{H}$ has the forms

$$|\rangle = \begin{pmatrix} |1\rangle \\ |2\rangle \end{pmatrix} = \begin{pmatrix} \rho_1 |A_1\rangle \\ \rho_2 |A_2\rangle \end{pmatrix}, \tag{2}$$

where ρ_1, ρ_2 are parameters to be determined, $|1\rangle$ and $|2\rangle$ are wave functions of the two levels. $|A_1\rangle, |A_2\rangle$ have the form

$$|A_1\rangle = \exp\left[\sum_{\mathbf{k}} \alpha_1(\mathbf{k}) a_{\mathbf{k}}^{\dagger}\right]|0\rangle, \tag{3}$$

$$|A_2\rangle = \exp\left[\sum_{\mathbf{k}} \alpha_2(\mathbf{k}) a_{\mathbf{k}}^{\dagger}\right]|0\rangle, \tag{4}$$

where $|0\rangle$ denotes the vacuum state of all the phonon modes, $\alpha_i(\mathbf{k})$ is the eigenvalue of $a_{\mathbf{k}}$ with $a_{\mathbf{k}}|A_i\rangle = \alpha_i(\mathbf{k})|A_i\rangle$, $i = 1,2$. The average number of all modes interacting with each level is

$$N_1 = \frac{\langle 1|\sum_{\mathbf{k}} a_{\mathbf{k}}^{\dagger} a_{\mathbf{k}}|1\rangle}{\langle 1|1\rangle} = \sum_{\mathbf{k}} |\alpha_1(\mathbf{k})|^2, \tag{5}$$

$$N_2 = \frac{\langle 2|\sum_{\mathbf{k}} a_{\mathbf{k}}^{\dagger} a_{\mathbf{k}}|2\rangle}{\langle 2|2\rangle} = \sum_{\mathbf{k}} |\alpha_2(\mathbf{k})|^2, \tag{6}$$

and $N = N_1 + N_2$ denotes the average total number that the phonon bath interact with the two-level system. The interaction energy of each level interacting with the phonon bath is defined as

TABLE I. Ground-state energy calculated by different methods for $S = 0.02$, 2, and 200.

δ_0/s	$E_{\mathrm{CA}(2)}/S$	E_{exact}/S	$E_{\mathrm{CCA}(4)}/S$	$E_{\mathrm{Lanczos}(3\times3)}/S$	$E_{\mathrm{CMX}(3)}/S$	$E_{\mathrm{AMX}(3)}/S$
			$S = 0.02$			
0.01	−1.009608	−1.009608	−1.009605	−1.009414	−1.009600	−1.009590
0.04	−1.038434	−1.038434	−1.038429	−1.038240	−1.038403	−1.038362
0.07	−1.067263	−1.067263	−1.067257	−1.067069	−1.067208	−1.067138
0.1	−1.096095	−1.096094	−1.096087	−1.095901	−1.096016	−1.095917
0.4	−1.384557	−1.384553	−1.384535	−1.384366	−1.384252	−1.383871
0.7	−1.673279	−1.673272	−1.673244	−1.673089	−1.672763	−1.672124
1.0	−1.962251	−1.962242	−1.962204	−1.962064	−1.961538	−1.960663
4.0	−4.864129	−4.864106	−4.864013	−4.863967	−4.862069	−4.859701
7.0	−7.783939	−7.783913	−7.783804	−7.783802	−7.781250	−7.778347
10.0	−10.717225	−10.717200	−10.717092	−10.717111	−10.714286	−10.711294
			$S = 2.0$			
0.01	−1.000100	−1.000212	−1.000029	−0.745727	−0.971538	−0.749238
0.04	−1.001590	−1.001204	−1.000470	−0.749580	−0.902069	−0.565450
0.07	−1.004809	−1.002728	−1.001438	−0.754338	−0.851250	−0.527121
0.1	−1.009641	−1.004789	−1.002935	−0.759994	−0.814286	−0.519989
0.4	−1.116919	−1.055737	−1.047042	−0.863116	−0.784615	−0.684991
0.7	−1.276675	−1.164368	−1.144520	−1.036099	−0.963158	−0.920463
1.0	−1.457427	−1.330803	−1.295572	−1.255278	−1.200000	−1.178257
4.0	−4.067366	−4.067174	−4.059590	−4.065555	−4.058824	−4.058081
7.0	−7.037148	−7.037131	−7.035658	−7.036839	−7.034483	−7.034327
10.0	−10.025677	−10.025673	−10.025166	−10.025575	−10.024390	−10.024334
			$S = 200.0$			
0.01	−1.000050	−1.000025	−1.000025	−0.117091	−0.210000	−0.031778
0.04	−1.000801	−1.000401	−1.000401	−0.122915	−0.098824	−0.061906
0.07	−1.002450	−1.001227	−1.001227	−0.135064	−0.104483	−0.093077
0.1	−1.004988	−1.002503	−1.002503	−0.152081	−0.124390	−0.119670
0.4	−1.074619	−1.040051	−1.040051	−0.413028	−0.406211	−0.406117
0.7	−1.203926	−1.122659	−1.122654	−0.706274	−0.703559	−0.703541
1.0	−1.366556	−1.250336	−1.250266	−1.003880	−1.002494	−1.002488
4.0	−4.000732	−4.000732	−3.991809	−4.000798	−4.000625	−4.000625
7.0	−7.000387	−7.000387	−6.998948	−7.000384	−7.000357	−7.000357
10.0	−10.000264	−10.000264	−9.999807	−10.000262	−10.000250	−10.000250

$$E_{b1}=\frac{\langle 1|\sum_{\mathbf{k}} g_{\mathbf{k}}(a_{\mathbf{k}}^{\dagger}+a_{\mathbf{k}})|1\rangle}{\langle 1|1\rangle}=\sum_{\mathbf{k}} g_{\mathbf{k}}[\alpha_1^{*}(\mathbf{k})+\alpha_1(\mathbf{k})], \tag{7}$$

$$E_{b2}=-\frac{\langle 2|\sum_{\mathbf{k}} g_{\mathbf{k}}(a_{\mathbf{k}}^{\dagger}+a_{\mathbf{k}})|2\rangle}{\langle 2|2\rangle}=-\sum_{\mathbf{k}} g_{\mathbf{k}}[\alpha_2^{*}(\mathbf{k})+\alpha_2(\mathbf{k})], \tag{8}$$

and $E_b=E_{b1}+E_{b2}$ is the total interaction energy of the system. It is easy to see that $|A_1\rangle,|A_2\rangle$ have relations

$$|A_1\rangle=\exp\left\{\sum_{\mathbf{k}} [\alpha_1(\mathbf{k})-\alpha_2(\mathbf{k})]a_{\mathbf{k}}^{\dagger}\right\}|A_2\rangle, \tag{9}$$

$$|A_2\rangle=\exp\left\{\sum_{\mathbf{k}} [\alpha_2(\mathbf{k})-\alpha_1(\mathbf{k})]a_{\mathbf{k}}^{\dagger}\right\}|A_1\rangle. \tag{10}$$

Substituting Eq. (2) into the Schrödinger equation

$$H|\rangle=E|\rangle \tag{11}$$

and utilizing the commutation relation $[a_{\alpha},a_{\beta}^{\dagger}]=\delta_{\alpha\beta}$, we get

$$E\rho_1|A_1\rangle=-\delta_0\rho_2|A_2\rangle+\rho_1\sum_{\mathbf{k}} \alpha_1(\mathbf{k})a_{\mathbf{k}}^{\dagger}|A_1\rangle + \rho_1\sum_{\mathbf{k}} g_{\mathbf{k}}a_{\mathbf{k}}^{\dagger}|A_1\rangle+\rho_1\sum_{\mathbf{k}} g_{\mathbf{k}}\alpha_1(\mathbf{k})|A_1\rangle, \tag{12}$$

$$E\rho_2|A_2\rangle=-\delta_0\rho_1|A_1\rangle+\rho_2\sum_{\mathbf{k}} \alpha_2(\mathbf{k})a_{\mathbf{k}}^{\dagger}|A_2\rangle - \rho_2\sum_{\mathbf{k}} g_{\mathbf{k}}a_{\mathbf{k}}^{\dagger}|A_2\rangle-\rho_2\sum_{\mathbf{k}} g_{\mathbf{k}}\alpha_2(\mathbf{k})|A_2\rangle, \tag{13}$$

where E is the eigenvalue of the ground-state energy. In Eqs. (14) and (15), we also omit two and higher correlation terms and take approximately

$$|A_1\rangle=\exp\left\{\sum_{\mathbf{k}} [\alpha_1(\mathbf{k})-\alpha_2(\mathbf{k})]a_{\mathbf{k}}^{\dagger}\right\}|A_2\rangle \approx\left\{1+\sum_{\mathbf{k}} [\alpha_1(\mathbf{k})-\alpha_2(\mathbf{k})]a_{\mathbf{k}}^{\dagger}\right\}|A_2\rangle, \tag{14}$$

$$|A_2\rangle=\exp\left\{\sum_{\mathbf{k}} [\alpha_2(\mathbf{k})-\alpha_1(\mathbf{k})]a_{\mathbf{k}}^{\dagger}\right\}|A_1\rangle \approx\left\{1+\sum_{\mathbf{k}} [\alpha_2(\mathbf{k})-\alpha_1(\mathbf{k})]a_{\mathbf{k}}^{\dagger}\right\}|A_1\rangle. \tag{15}$$

From Eqs. (12)–(15) and equating the coefficients of $|A_i\rangle$, $a_{\mathbf{k}}^{\dagger}|A_i\rangle$ $(i=1,2)$ in Eqs. (12) and (13), we have

TABLE II. Ground-state energy calculated by different methods for $\delta_0=0.01$, 1, and 100.

δ_0/s	$E_{\mathrm{CA}(2)}/S$	E_{exact}	$E_{\mathrm{CCA}(4)}/S$
		$\delta_0=0.01$	
0.01	−1.009804	−1.009804	−1.009804
0.04	−1.039216	−1.039216	−1.039216
0.07	−1.068628	−1.068628	−1.068628
0.1	−1.098041	−1.098041	−1.098041
0.4	−1.392187	−1.392187	−1.392187
0.7	−1.686367	−1.686366	−1.686365
1.0	−1.980581	−1.980579	−1.980574
4.0	−4.924589	−4.924512	−4.924060
7.0	−7.872005	−7.871596	−7.867917
10.0	−10.822841	−10.821663	−10.806535
		$\delta_0=1$	
0.01	−1.003341	−1.003341	−1.003341
0.04	−1.013454	−1.013453	−1.013449
0.07	−1.023708	−1.023704	−1.023683
0.1	−1.034109	−1.034098	−1.034033
0.4	−1.147920	−1.146829	−1.141923
0.7	−1.289023	−1.279103	−1.251728
1.0	−1.500000	−1.436545	−1.375042
4.0	−4.142857	−4.067461	−4.067031
7.0	−7.076923	−7.037096	−7.037094
10.0	−10.052632	−10.025659	−10.025659
		$\delta_0=100$	
0.01	−1.000050	−1.000050	−1.000050
0.04	−1.000203	−1.000203	−1.000202
0.07	−1.000361	−1.000361	−1.000350
0.1	−1.000525	−1.000525	−1.000478
0.4	−1.002734	−1.002726	−0.991066
0.7	−1.140393	−1.058663	−1.057693
1.0	−1.367092	−1.250674	−1.250598
4.0	−4.121464	−4.062539	−4.062539
7.0	−7.070764	−7.035727	−7.035727
10.0	−10.049777	−10.025006	−10.025006

$$E\rho_1=-\delta_0\rho_2+\rho_1\sum_{\mathbf{k}} g_{\mathbf{k}}\alpha_1(\mathbf{k}), \tag{16}$$

$$E\rho_2=-\delta_0\rho_1+\rho_2\sum_{\mathbf{k}} g_{\mathbf{k}}\alpha_2(\mathbf{k}), \tag{17}$$

$$0=-\delta_0\rho_2\sum_{\mathbf{k}} [\alpha_2(\mathbf{k})-\alpha_1(\mathbf{k})]+\rho_1\sum_{\mathbf{k}} \alpha_1(\mathbf{k})+\rho_1\sum_{\mathbf{k}} g_{\mathbf{k}}, \tag{18}$$

$$0=-\delta_0\rho_1\sum_{\mathbf{k}} [\alpha_1(\mathbf{k})-\alpha_2(\mathbf{k})]+\rho_2\sum_{\mathbf{k}} \alpha_2(\mathbf{k})-\rho_2\sum_{\mathbf{k}} g_{\mathbf{k}}. \tag{19}$$

Then the analytical solutions under the first level approximation can be easily obtained:

$$E=-s+\left(r-\frac{2r^2s}{\delta_0 r^2+r+\delta_0}\right)\delta_0, \tag{20}$$

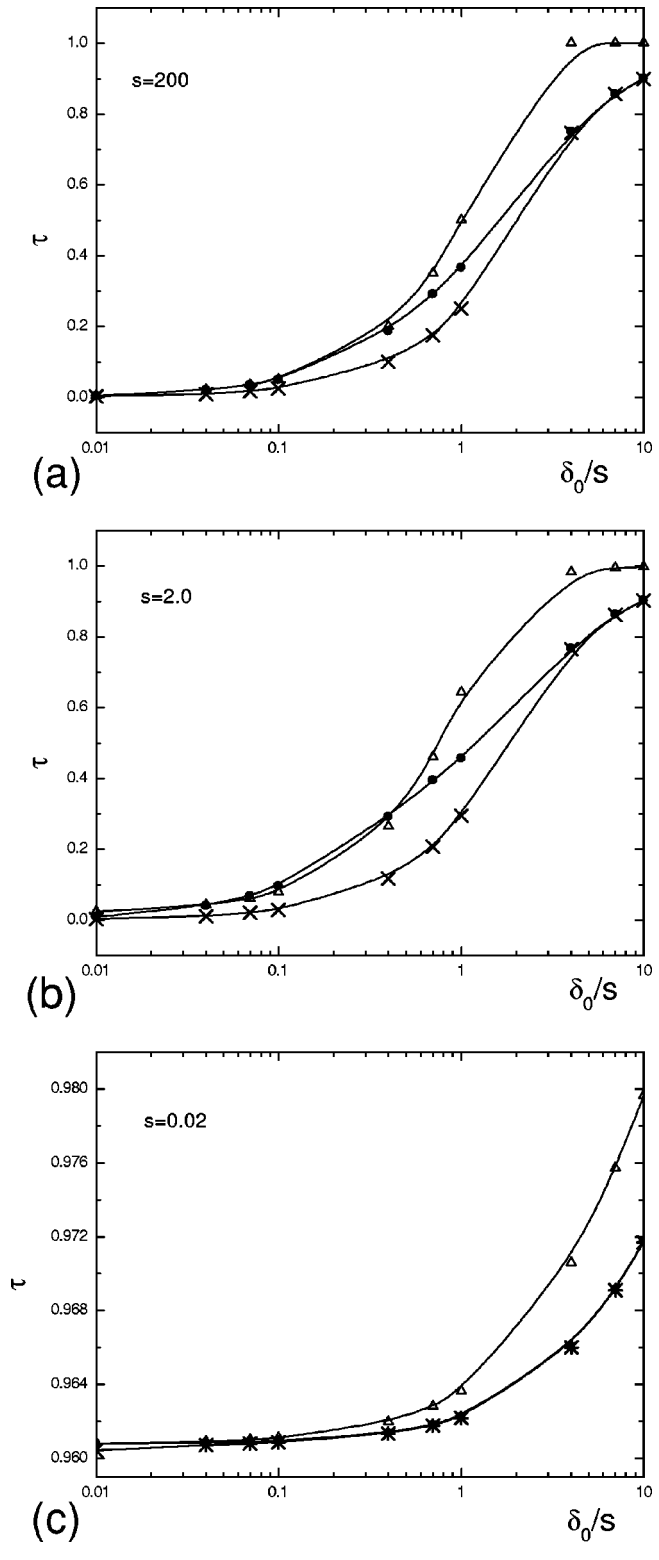

FIG. 1. Tunneling reduction factor τ_{CA} versus δ_0 for $s=$(a) 200, (b) 2.0, (c) 0.02. The lines with ●, ×, and △ represent $\tau_{\mathrm{CA}}^{(2)}$, $\tau_{\mathrm{CCA}}^{(4)}$, and τ_{exact}, respectively.

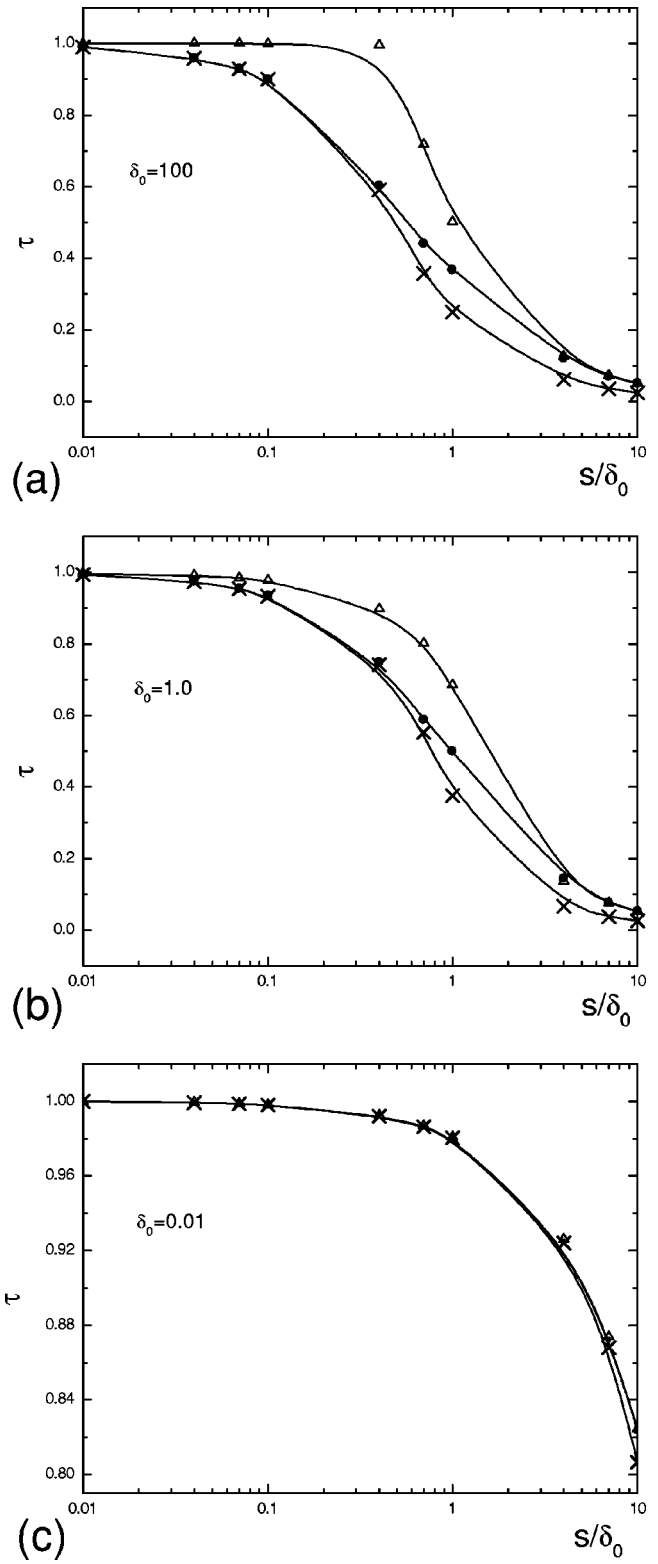

FIG. 2. Tunneling reduction factor τ_{CA} versus s for $\delta_0=$(a) 100, (b) 1.0, (c) 0.01. The lines with ●, ×, and △ represent $\tau_{\mathrm{CA}}^{(2)}$, $\tau_{\mathrm{CCA}}^{(4)}$, and τ_{exact}, respectively.

$$r=\frac{2s-1\pm\sqrt{(2s-1)^2-4\delta_0^2}}{2\delta_0} \quad \text{or} \quad r=\pm 1, \tag{21}$$

$$\alpha_1(\mathbf{k})=\frac{\delta_0 r^2-\delta_0-r}{\delta_0 r^2+\delta_0+r}g_{\mathbf{k}}, \tag{22}$$

$$\alpha_2(\mathbf{k})=\frac{\delta_0 r^2-\delta_0+r}{\delta_0 r^2+\delta_0+r}g_{\mathbf{k}}, \tag{23}$$

where $r=\rho_2/\rho_1$, $s=\Sigma_{\mathbf{k}}g_{\mathbf{k}}^2$. It is clear that the ground-state energies (20) for the first-level CA equal to $E_0=-\delta_0$ when

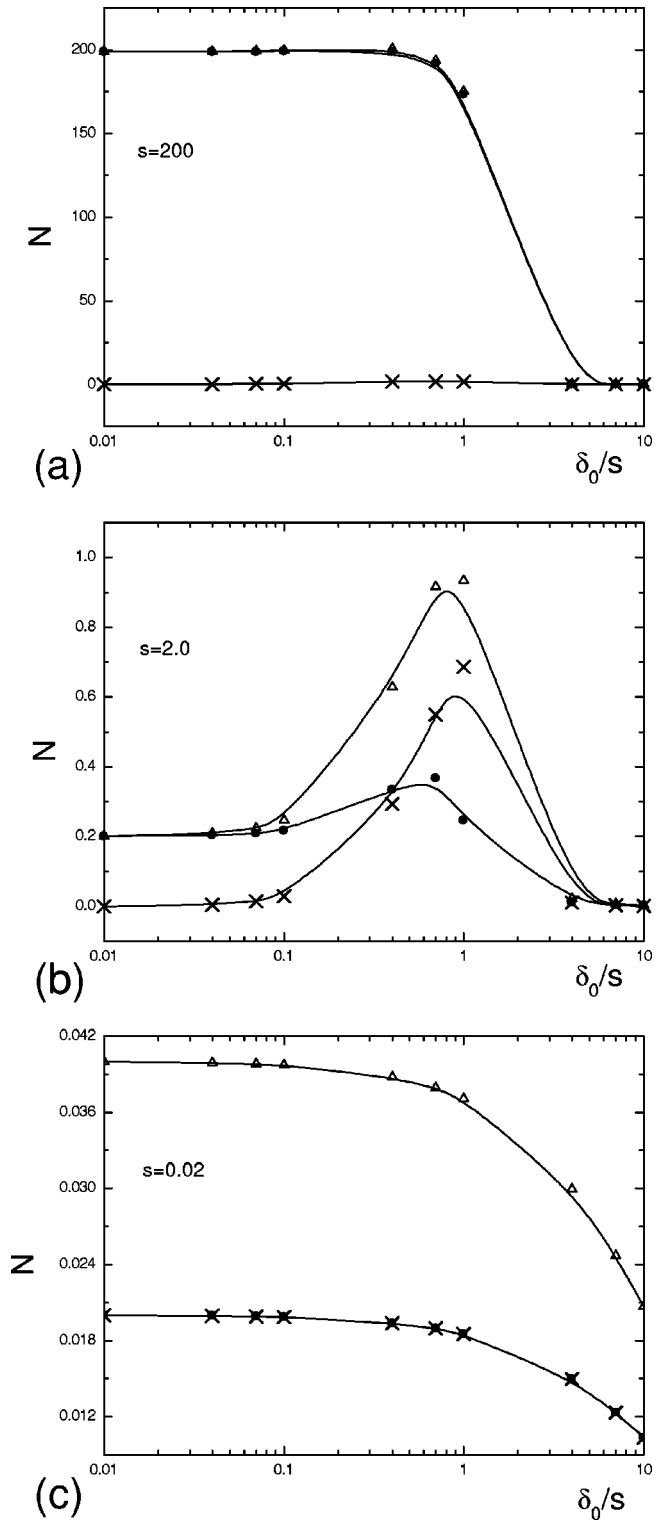

FIG. 3. Interaction phonon numbers N versus δ_0 for $s=$(a) 200, (b) 2.0, (c) 0.02. The lines with ●, ×, and △ represent N_1, N_2, and N, respectively.

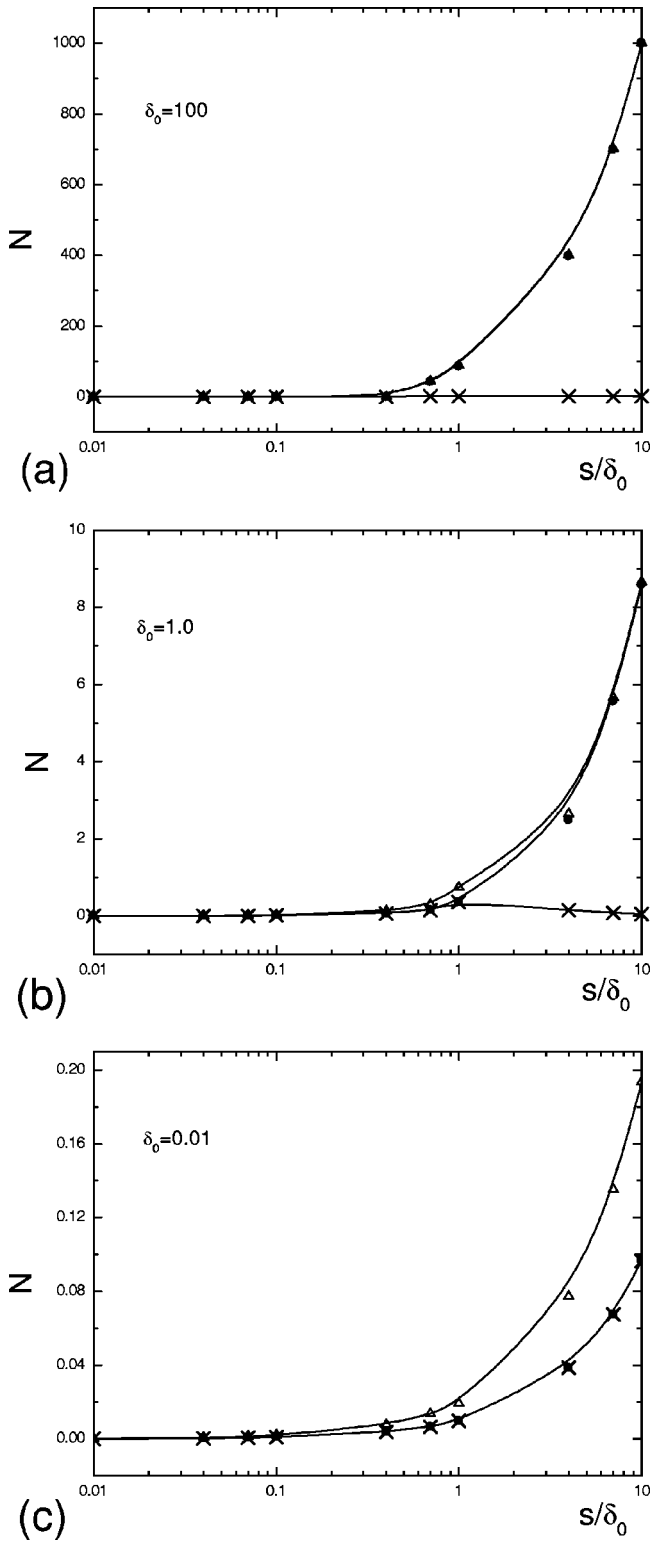

FIG. 4. Interaction phonon numbers N versus s for $\delta_0=$(a) 100, (b) 1.0, (c) 0.01. The lines with ●, ×, and △ represent N_1, N_2, and N, respectively.

the system is uncoupled ($g_{\mathbf{k}}=0$). The tunneling reduction faction $\tau_{CA}^{(1)}$ can be defined as

$$\tau_{CA}^{(1)}=r-\frac{2r^2}{\delta_0 r^2+r+\delta_0}. \tag{24}$$

In the second level of the approximation we include in the ground-state wave function the effect of two-phonon correlations and calculate the ground state more accurately. The higher-order correlation terms, which are relatively small, are omitted:

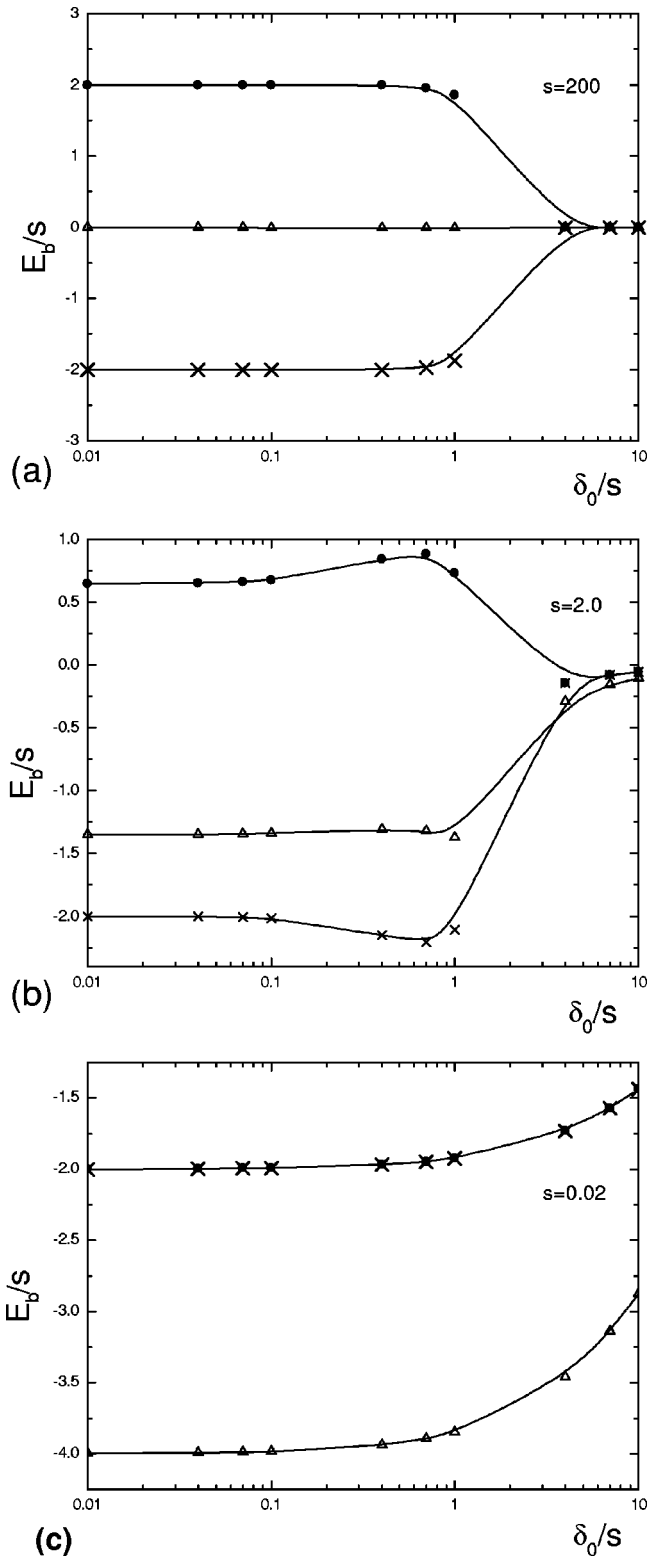

FIG. 5. Interaction energy E_b versus δ_0 for $s=$(a) 200, (b) 2.0, (c) 0.02. The lines with ●, ×, and △ represent E_{b1}, E_{b2}, and E_b, respectively.

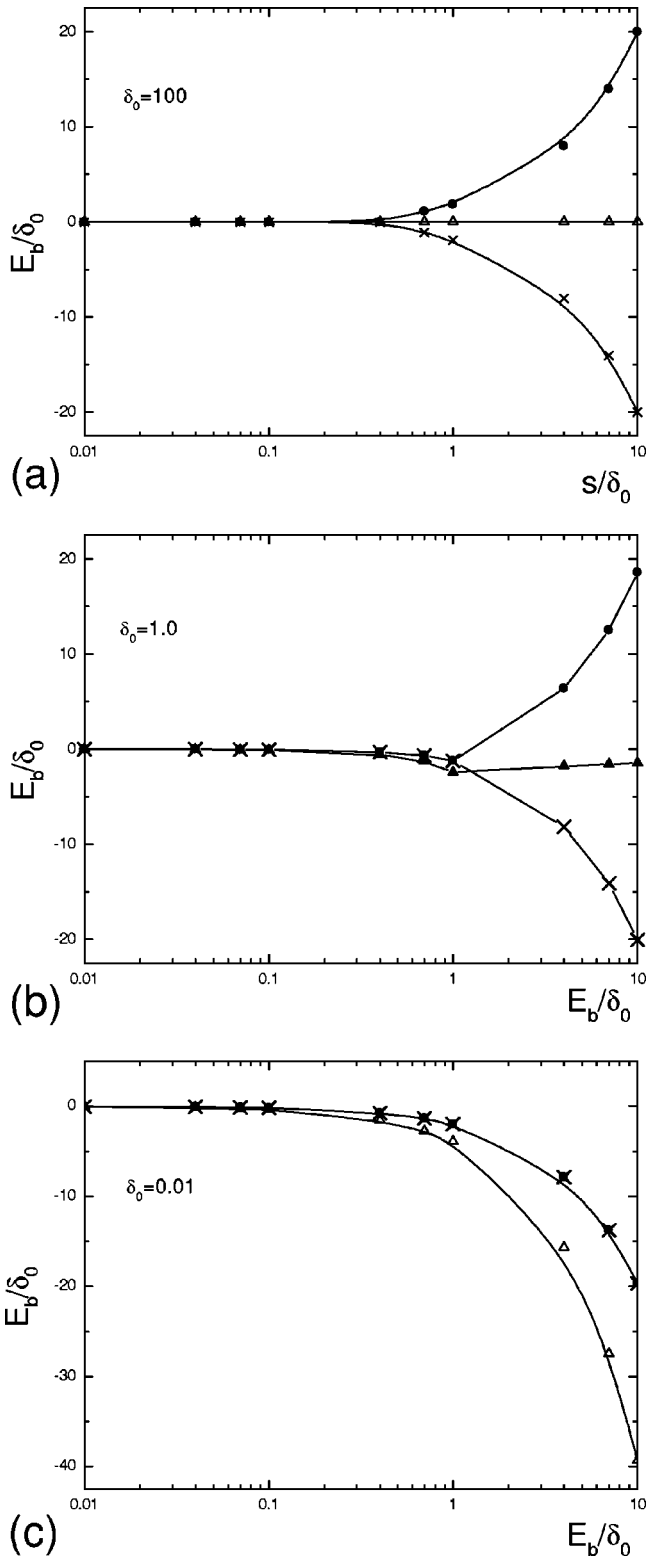

FIG. 6. Interaction energy E_b versus s for $\delta_0=$(a) 100, (b) 1.0, (c) 0.01. The lines with ●, ×, and △ represent E_{b1}, E_{b2}, and E_b, respectively.

$$|\rangle=\begin{pmatrix}|1\rangle\\|2\rangle\end{pmatrix}=\begin{pmatrix}\left[\rho_1+\sum_{\mathbf{k}_1,\mathbf{k}_2} f_1(\mathbf{k}_1,\mathbf{k}_2)a^\dagger_{\mathbf{k}_1}a^\dagger_{\mathbf{k}_2}\right]|A_1\rangle\\\left[\rho_2+\sum_{\mathbf{k}_1,\mathbf{k}_2} f_2(\mathbf{k}_1,\mathbf{k}_2)a^\dagger_{\mathbf{k}_1}a^\dagger_{\mathbf{k}_2}\right]|A_2\rangle\end{pmatrix}, \tag{25}$$

where $\rho_1,\rho_2,f_1(\mathbf{k}_1,\mathbf{k}_2),f_2(\mathbf{k}_1,\mathbf{k}_2)$ are functions to be determined. $|A_1\rangle$ and $|A_2\rangle$ are the same as Eqs. (3) and (4) and the relation of $|A_1\rangle$ and $|A_2\rangle$ are expanded approximately to the second level $a^\dagger_{\mathbf{k}_1}a^\dagger_{\mathbf{k}_2}|A_i\rangle$ $(i=1,2)$ rather by the use of Eqs. (14) and (15):

$$|A_1\rangle \approx \left\{ 1+\sum_{\mathbf{k}} [\alpha_1(\mathbf{k})-\alpha_2(\mathbf{k})]a_{\mathbf{k}}^{\dagger} + \frac{1}{2}\sum_{\mathbf{k}_1,\mathbf{k}_2} [\alpha_1(\mathbf{k}_1)-\alpha_2(\mathbf{k}_1)][\alpha_1(\mathbf{k}_2)-\alpha_2(\mathbf{k}_2)]a_{\mathbf{k}_1}^{\dagger}a_{\mathbf{k}_2}^{\dagger} \right\} |A_2\rangle, \tag{26}$$

$$|A_2\rangle \approx \left\{ 1+\sum_{\mathbf{k}} [\alpha_2(\mathbf{k})-\alpha_1(\mathbf{k})]a_{\mathbf{k}}^{\dagger} + \frac{1}{2}\sum_{\mathbf{k}_1,\mathbf{k}_2} [\alpha_2(\mathbf{k}_1)-\alpha_1(\mathbf{k}_1)][\alpha_2(\mathbf{k}_2)-\alpha_1(\mathbf{k}_2)]a_{\mathbf{k}_1}^{\dagger}a_{\mathbf{k}_2}^{\dagger} \right\} |A_1\rangle. \tag{27}$$

Substituting Eq. (25) in the Schrödinger equation (11) and equating the coefficients of $|A_i\rangle, a_{\mathbf{k}}^{\dagger}|A_i\rangle, a_{\mathbf{k}_1}^{\dagger}a_{\mathbf{k}_2}^{\dagger}|A_i\rangle$ $(i=1,2)$, in the corresponding equations yields

$$E = -s-\delta_0 r + \frac{2\delta_0 r^2 - 2rP_1}{\delta_0 r^2 + (1-P_1)r + \delta_0 - P_2}, \tag{28}$$

$$P_1 = \frac{(\delta_0 r^2 + r + \delta_0) \pm \sqrt{(\delta_0 r^2 + r + \delta_0)^2 - \dfrac{8s\delta_0 r^2 (r^2 + 2\delta_0 r + 1)}{\delta_0(1+r^2)+2r}}}{r^2 + 2\delta_0 r + 1} \frac{\delta_0 + r}{2}, \tag{29}$$

$$P_2 = \frac{\delta_0 r + 1}{\delta_0 + r} P_1. \tag{30}$$

Here r satisfies a simple equation

$$\begin{aligned} &-\delta_0 r^4 + (2\delta_0 s - \delta_0 + \delta_0 P_1) r^3 + (\delta_0 P_2 - 2P_1 s) r^2 \\ &\quad + (\delta_0 - \delta_0 P_1 + 2P_2 s - 2\delta_0 s) r + (\delta_0^2 - P_2 \delta_0) \\ &\quad = 0 \end{aligned} \tag{31}$$

and can be evaluated numerically for given s and δ_0. The corresponding interaction phonon numbers and the interaction energies in the second-level approximation are

$$N_1 = \left(\frac{Ca_1}{Ca}\right)^2 s + \frac{4s^2 r^3 \delta_0 (\delta_0 + r) Ca_1^2}{[\delta_0(1+r^2)+2r]Ca^4 + 2\delta_0 s^2 r^3 (\delta_0 + r) Ca_1^2}, \tag{32}$$

$$N_2 = \left(\frac{Ca_2}{Ca}\right)^2 s + \frac{4s^2 r^2 \delta_0 (\delta_0 r + 1) Ca_2^2}{[\delta_0(1+r^2)+2r]Ca^4 + 2\delta_0 s^2 r^2 (\delta_0 r + 1) Ca_2^2}, \tag{33}$$

$$N = N_1 + N_2, \tag{34}$$

$$E_{b1} = 2s\frac{Ca_1}{Ca} + \frac{4\delta_0 s^2 r^3 (\delta_0 + r) Ca_1 Ca}{[\delta_0(1+r^2)+2r]Ca^4 + 2\delta_0 s^2 r^3 (\delta_0 + r) Ca_1^2}, \tag{35}$$

$$E_{b2} = -2s\frac{Ca_2}{Ca} - \frac{4\delta_0 s^2 r^2 (\delta_0 r + 1) Ca_2 Ca}{[\delta_0(1+r^2)+2r]Ca^4 + 2\delta_0 s^2 r^2 (\delta_0 r + 1) Ca_2^2}, \tag{36}$$

$$E_b = E_{b1} + E_{b2}, \tag{37}$$

where

$$Ca_1 = P_2 + \delta_0 r^2 - \delta_0 - r - rP_1, \tag{38}$$

$$Ca_2 = P_2 + \delta_0 r^2 - \delta_0 + r - rP_1, \tag{39}$$

$$Ca = -P_2 + \delta_0 r^2 + \delta_0 + r - rP_1. \tag{40}$$

Finally, following the same idea as shown above, the correlation terms whose order higher than three are omitted and the ground-state wave function for the third level CA can be written as

$$|\rangle = \begin{pmatrix} \left[\rho_1 + \sum_{\mathbf{k}_1,\mathbf{k}_2} f_1(\mathbf{k}_1,\mathbf{k}_2) a_{\mathbf{k}_1}^{\dagger}a_{\mathbf{k}_2}^{\dagger} + \sum_{\mathbf{k}_1,\mathbf{k}_2,\mathbf{k}_3} \beta_1(\mathbf{k}_1,\mathbf{k}_2,\mathbf{k}_3) a_{\mathbf{k}_1}^{\dagger}a_{\mathbf{k}_2}^{\dagger}a_{\mathbf{k}_3}^{\dagger}\right]|A_1\rangle \\ \left[\rho_2 + \sum_{\mathbf{k}_1,\mathbf{k}_2} f_2(\mathbf{k}_1,\mathbf{k}_2) a_{\mathbf{k}_1}^{\dagger}a_{\mathbf{k}_2}^{\dagger} + \sum_{\mathbf{k}_1,\mathbf{k}_2,\mathbf{k}_3} \beta_2(\mathbf{k}_1,\mathbf{k}_2,\mathbf{k}_3) a_{\mathbf{k}_1}^{\dagger}a_{\mathbf{k}_2}^{\dagger}a_{\mathbf{k}_3}^{\dagger}\right]|A_2\rangle \end{pmatrix} \tag{41}$$

TABLE III. Ground-state energy calculated by CA in the different level approximations for $S=0.02$.

δ_0/s	$E_{\mathrm{CA}(1)}/S$	$E_{\mathrm{CA}(2)}/S$	$E_{\mathrm{CA}(3)}/S$	$\tau_{\mathrm{CA}}^{(3)}$	$E_{b(3)}/s$	E_{exact}/S	τ_{exact}
0.01	−1.009600	−1.009608	−1.009608	0.960804	−0.999608	−1.009608	0.960820
0.04	−1.038403	−1.038434	−1.038434	0.960850	−0.998434	−1.038434	0.960910
0.07	−1.067208	−1.067263	−1.067263	0.960895	−0.997263	−1.067263	0.961000
0.1	−1.096016	−1.096095	−1.096094	0.960940	−0.996094	−1.096094	0.961089
0.4	−1.384252	−1.384557	−1.384553	0.961383	−0.984553	−1.384553	0.961968
0.7	−1.672763	−1.673279	−1.673272	0.961817	−0.973272	−1.673272	0.962819
1.0	−1.961539	−1.962251	−1.962242	0.962242	−0.962242	−1.962242	0.963641
4.0	−4.862069	−4.864129	−4.864106	0.966027	−0.864106	−4.864106	0.970575
7.0	−7.781250	−7.783939	−7.783913	0.969130	−0.783917	−7.783913	0.975719
10.0	−10.714286	−10.717225	−10.717200	0.971720	−0.717200	−10.717200	0.979635

and the approximate relation between $|A_1\rangle$ and $|A_2\rangle$ can be written as

$$
\begin{aligned}
|A_1\rangle \approx \Bigg\{ & 1+\sum_{\mathbf{k}} [\alpha_1(\mathbf{k})-\alpha_2(\mathbf{k})]a_{\mathbf{k}}^{\dagger} \\
& +\frac{1}{2}\sum_{\mathbf{k}_1,\mathbf{k}_2} [\alpha_1(\mathbf{k}_1)-\alpha_2(\mathbf{k}_1)] \\
& \times[\alpha_1(\mathbf{k}_2)-\alpha_2(\mathbf{k}_2)]a_{\mathbf{k}_1}^{\dagger}a_{\mathbf{k}_2}^{\dagger} \\
& +\frac{1}{6}\sum_{\mathbf{k}_1,\mathbf{k}_2,\mathbf{k}_3} [\alpha_1(\mathbf{k}_1)-\alpha_2(\mathbf{k}_1)][\alpha_1(\mathbf{k}_2)-\alpha_2(\mathbf{k}_2)] \\
& \times[\alpha_1(\mathbf{k}_3)-\alpha_2(\mathbf{k}_3)]a_{\mathbf{k}_1}^{\dagger}a_{\mathbf{k}_2}^{\dagger}a_{\mathbf{k}_3}^{\dagger}\Bigg\}|A_2\rangle, \qquad (42)
\end{aligned}
$$

$$
\begin{aligned}
|A_2\rangle \approx \Bigg\{ & 1+\sum_{\mathbf{k}} [\alpha_2(\mathbf{k})-\alpha_1(\mathbf{k})]a_{\mathbf{k}}^{\dagger} \\
& +\frac{1}{2}\sum_{\mathbf{k}_1,\mathbf{k}_2} [\alpha_2(\mathbf{k}_1)-\alpha_1(\mathbf{k}_1)] \\
& \times[\alpha_2(\mathbf{k}_2)-\alpha_1(\mathbf{k}_2)]a_{\mathbf{k}_1}^{\dagger}a_{\mathbf{k}_2}^{\dagger} \\
& +\frac{1}{6}\sum_{\mathbf{k}_1,\mathbf{k}_2,\mathbf{k}_3} [\alpha_2(\mathbf{k}_1)-\alpha_1(\mathbf{k}_1)][\alpha_2(\mathbf{k}_2)-\alpha_1(\mathbf{k}_2)] \\
& \times[\alpha_2(\mathbf{k}_3)-\alpha_1(\mathbf{k}_3)]a_{\mathbf{k}_1}^{\dagger}a_{\mathbf{k}_2}^{\dagger}a_{\mathbf{k}_3}^{\dagger}\Bigg\}|A_1\rangle. \qquad (43)
\end{aligned}
$$

The resultant expressions are very lengthy and will not be presented here. Following the same way we took in the first and the second level approximation, the energy E and other physical quantities can be obtained.

It should be noted that we can systematically improve the approximation of the results by including more higher level correlations. In Sec. III, we will see that the results of the two-level approximation are close enough to the exact solutions. So there is no need to take higher level CA. This also shows the efficiency of our method.

III. NUMERICAL RESULTS AND DISCUSSION

In Tables I and II, we show the ground-state energies calculated by the coupled-cluster approximation (E_{CCA}), the Lanczos scheme (E_{Lanczos}), the connected moments expansion (E_{CMX}), the alternate moments expansion (E_{AMX}), and the exact numerical diagonalization (E_{exact}), as well as CA in the second-level approximation ($E_{\mathrm{CA}(2)}$). It is clear that $E_{\mathrm{CA}(2)}$ and E_{CCA} are better than E_{Lanczos}, E_{AMX}, and E_{CMX}, and show good agreement with the exact results. However, in the intermediate region $\delta_0 \approx s \approx \hbar\omega_0 \approx 1$, the results are not as good as those when δ_0 is far from s. The differences are a few percent. In some cases, $E_{\mathrm{CA}(2)}$ are lower than the exact results. This is because of that the CA is an unvariational approach. When more correlation terms are considered, the results will gradually approach the exact ones.

In Figs. 1 and 2, we plot the tunneling reduction factor $\tau_{\mathrm{CA}}^{(2)}$ versus δ_0 for $S=0.2,2,200$ and S for $\delta_0=0.01,1,100$. Our results show that there is no abrupt jump in the value of the reduction factor as δ_0 or s varies. These mean that there is no evidence of the discontinuous localization-delocalization transition. The results are consistent with those of the exact calculations and the CCA. Figures 1 and 2 also show that our reduction factor values $\tau_{\mathrm{CA}}^{(2)}$ are closer to the exact values than those of CCA for all cases. This may indicate that the CA can well simulate the ground state of the real system in the whole parameter space.

The numbers of phonons interacting with each level and the whole two-level system are shown in Figs. 3 and 4. As s increase, the system interacts with more phonons, i.e., the total phonon numbers N increases monotonically with s/δ_0. When $\delta_0=0.01$, both levels have the same phonons, whereas $\delta_0=1.0$ and 100 the level $|1\rangle$ will occupy most of the phonons if the coupling is strong enough ($s/\delta_0>1.0$). In Fig. 3(c) and 4(c), we show weak coupling situations where s is very small ($s\leqslant 0.1$). In this case, the two-level system is mainly controlled by the tunneling effect and the two levels almost have the same numbers of the interaction phonons. This also can be seen in Figs. 4(a) and 4(b) while $s/\delta_0 \leqslant 0.1$. The strong coupling situations are shown in Fig. 3(a), where $s=200$. When $\delta_0/s<1.0$ the coupling effect takes advantage and the level $|1\rangle$ tends to occupy more interaction phonons. But compared to the weak coupling cases, the numbers of the phonons in the level $|2\rangle$ still changes little. When δ_0/s increase, the tunneling effect becomes more important.

TABLE IV. Ground-state energy calculated by CA in the different level approximations for $\delta_0=0.01$.

s/δ_0	$E_{\mathrm{CA}(1)}/S$	$E_{\mathrm{CA}(2)}/S$	$E_{\mathrm{CA}(3)}/S$	$\tau_{\mathrm{CA}}^{(3)}$	$E_{b(3)}/s$	E_{exact}/S	τ_{exact}
0.01	−1.0098039	−1.0098039	−1.0098039	0.9998039	−0.9998039	−1.009804	0.999808
0.04	−1.0392157	−1.0392160	−1.0392160	0.9992160	−0.9992160	−1.039216	0.999231
0.07	−1.0686275	−1.0686284	−1.0686284	0.9986284	−0.9986284	−1.068628	0.998655
0.1	−1.0980392	−1.0980411	−1.0980411	0.9980411	−0.9980411	−1.098041	0.998079
0.4	−1.3921569	−1.3921870	−1.3921869	0.9921869	−0.9921869	−1.392187	0.992339
0.7	−1.6862745	−1.6863669	−1.6863665	0.9863665	−0.9863665	−1.686366	0.986630
1.0	−1.9803922	−1.9805807	−1.9805795	0.9805795	−0.9805795	−1.980579	0.980953
4.0	−4.9215686	−4.9245887	−4.9245101	0.9245101	−0.9245101	−4.924512	0.925882
7.0	−7.8627451	−7.8720048	−7.8715819	0.8715819	−0.8715819	−7.871596	0.873798
10.0	−10.8039216	−10.8228408	−10.8216041	0.8216041	−0.8216041	−10.821663	0.824552

Hence N_1 decrease quickly correspondingly and both levels tend to occupy the same numbers of phonons. While δ_0/s is close to 10, the interaction phonon numbers with two levels decrease asymptotically to zero.

In the intermediate coupling region where $\delta_0 \approx s$ in Fig. 3(b), the tunneling and coupling effect compete against each other and the peaks occur in the curves of interaction phonon numbers versus δ_0/s. This effect is the so-called strong nonlinear self-trapping effect. There is also a phenomenon of phonon number inversion near the point $\delta_0/s=0.5$ in Fig. 3(b). When $\delta_0/s<0.5$, the interaction phonons in the level $|1\rangle$ are more than in $|2\rangle$. As δ_0/s increases to $\delta_0/s\approx 0.5$, population inversion occurs. The numbers of the interaction phonons in the level $|2\rangle$ rise quickly and exceed the numbers in $|1\rangle$ thereafter.

In Figs. 5 and 6, we show interaction energy E_{b1}, E_{b2} for each level and the total interaction energy E_b for the system. In some cases, for example, $s=2.0,200$ and $\delta_0=1.0,100$, the interaction energies with level $|1\rangle$ have positive values. But the total interaction energies are still below zero and make the system stable. When s is small, the same interaction phonons in each level consequently leads to the similarity in the interaction energy for each level. In Figs. 6(a) and 6(b), the enhancement of the coupling effect make the interaction energy E_{b1} for the level $|1\rangle$ rise and E_{b2} for the level $|2\rangle$ decrease. But the interaction energy E_b for the whole system does not very much. It remains a little below zero in the whole parameter space. When δ_0/s reduce to zero, the tunneling effect becomes weak, hence the curves in Figs. 3 and 5 become flat. The saturation values for the interaction phonon numbers and the interaction energy turn close to the results of the systems which consist of a sets of oscillators.

As we stressed before, our method is not a variational one but rather a systemic approximation method. We show here some results of the third-level approximation. In Tables III and IV, we show the CA results for different level approximations. In Table III, the coupling parameter s is fixed to be 0.02, and the bare tunneling factor δ_0 varies. In Table IV, δ_0 is fixed to be 0.01 and s changes. It is clear that in the third-level approximation the ground-state energy $E_{\mathrm{CA}(3)}$ and the tunneling reduction factor $\tau_{\mathrm{CA}}^{(3)}$ are closer to the exact results obtained in Ref. 14. In fact, in most cases, both values are almost the same in the precision of 10^{-6}. The binding energy $E_{b(3)}$ is defined as $E_{b(3)}=E_{\mathrm{CA}(3)}-E_0=E_{\mathrm{CA}(3)}+\delta_0$.

In Fig. 7, we plot the ground-state energy E versus $1/N_{\mathrm{tr}}$ for $s=0.02$ and $\delta_0/s=1.0$ and 10.0, where N_{tr} is the truncation size of the CA. Extended the lines to the E axis, the E intercept may represent the ''infinite'' order truncation level for the CA. Obviously, the two intercept values are very close to the numerical ones. This also indicates the convergency and the validity for the CA.

IV. CONCLUSION

In this paper we have investigated the ground-state properties of a two-level system coupled to a dispersionless phonon bath by the coherent approximation. In the first level approximation, we considered the effect of the one-phonon correlation, and obtained analytic solutions which are much closer to the exact results than the ones obtained by the variational method. In the second level approximation, we took into account the effect of the two-phonon correlation and obtained very good energies and tunneling reduction factors. In our method, the interaction energies, the interaction phonon numbers of each level, and the whole two-level system, which depend on the bare tunneling matrix element δ_0 and coupling parameter s, are also calculated. The number of phonons in the level $|1\rangle$ is found to grow with s while that in

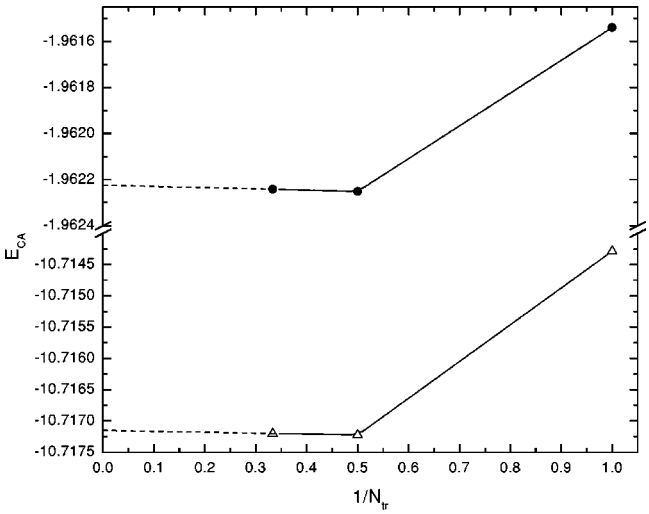

FIG. 7. Ground-state energy E versus $1/N_{\mathrm{tr}}$, for $s=0.02$. The lines with ● and △ represent $\delta 0/s=1.0$ and 10.0, respectively.

$|2\rangle$, does not vary much. In the intermediate coupling region $\delta_0 \approx s \approx 1$, we found a maximum value for the interaction phonon numbers versus δ_0/s and a phenomenon of population inversion. We also confirmed the conclusion that there is no discontinuous localization-delocalization transition for the system. This conclusion is obtained by the exact and CCA calculations, but is opposite to the prediction of the variational approach.

ACKNOWLEDGMENTS

This work was partially supported by the President Foundation of the Chinese Academy of Science.

*Corresponding author. Email address: klwang@ustc.edu.cn

[1] A.J. Leggett, S. Chakravarty, A.T. Dorsey, M.P.A. Fisher, A. Garg, and W. Zwerger, Rev. Mod. Phys. **59**, 1 (1987), and references therein; **67**, 725(E) (1995).
[2] H.B. Shore and L.M. Sander, Phys. Rev. B **7**, 4537 (1973).
[3] A. Zawadowski and G.T. Zimanyi, Phys. Rev. B **32**, 1373 (1985).
[4] R. Silbey and R.A. Harris, J. Chem. Phys. **80**, 2615 (1984).
[5] A. Tanaka and A. Sakurai, Prog. Theor. Phys. **76**, 999 (1986).
[6] H. Chen, Y.M. Zhang, and X. Wu, Phys. Rev. B **40**, 11 326 (1989).
[7] A.M. Jayannavar, Solid State Commun. **71**, 689 (1989).
[8] Y. Zhang, H. Chen, and X. Wu, J. Phys. C **2**, 3119 (1990); Phys. Rev. B **41**, 11 600 (1990).
[9] C.F. Lo and R. Sollie, Phys. Rev. B **44**, 5013 (1991).
[10] B. Dutta and A.M. Jayannavar, Phys. Rev. B **49**, 3604 (1994).
[11] T.P. Pareek and A.M. Jayannavar, Int. J. Mod. Phys. B **9**, 1343 (1995).
[12] Z. Ivić, D. Kapor, G. Vujičić, and A. Tančić, Phys. Lett. A **172**, 461 (1993).
[13] C.F. Lo and W.H. Wong, Phys. Rev. B **52**, 3333 (1995).
[14] C.F. Lo and W.H. Wong, Chem. Phys. Lett. **256**, 159 (1996).
[15] Vassilios Fessatidis, Jay D. Mancini, William J. Massano, and Samuel P. Bowen, Phys. Rev. B **61**, 3184 (2000).
[16] J.D. Mancini, Y. Zhou, and P.F. Meier, Phys. Lett. A **185**, 435 (1994).
[17] J.D. Mancini, Y. Zhou, and P.F. Meier, Int. J. Quantum Chem. **50**, 101 (1994).
[18] W.H. Wong and C.F. Lo, Phys. Rev. B **54**, 12 859 (1996).
[19] T.A. Costi and C. Kieffer, Phys. Rev. Lett. **76**, 1683 (1996).
[20] S. Chakravarty and J. Rudnick, Phys. Rev. Lett. **75**, 501 (1995).
[21] C.F. Lo, E. Manousakis, R. Sollie, and Y.L. Wang, Phys. Rev. B **50**, 418 (1994).
[22] C.F. Lo and R. Sollie, Phys. Rev. A **47**, 733 (1993).
[23] D.N. Zubarev, Usp. Fiz. Nauk **71**, 71 (1960) [Sov. Phys. Usp. **3**, 320 (1960)].